Available online at www.sciencedirect.com
SCIENCE DIRECT®
Journal of the European Ceramic Society 25 (2005) 455–462
www.elsevier.com/locate/jeurceramsoc

Submicrometric NASICON ceramics with improved electrical conductivity obtained from mechanically activated precursors

R. O. Fuentes [a,b], F. M. Figueiredo [b,c,*], M. R. Soares [d], F. M. B. Marques [b]

[a] *CINSO-CITEFA-CONICET, J.B. de la Salle 4397, B1603ALO Villa Martelli, Buenos Aires, Argentina*
[b] *Department of Ceramics and Glass Engineering, CICECO, University of Aveiro, 3810-193 Aveiro, Portugal*
[c] *Science and Technology Department, Universidade Aberta, 1269-001 Lisbon, Portugal*
[d] *Laboratório Central de Análises, University of Aveiro, 3810-193 Aveiro, Portugal*

Received 5 December 2003; received in revised form 20 February 2004; accepted 25 February 2004
Available online 21 July 2004

Abstract

$Na_3Si_2Zr_{1.88}Y_{0.12}PO_{11.94}$ was for the first time synthesised using mechanically activated mixtures of $(ZrO_2)_{0.97}(Y_2O_3)_{0.03}$, $Na_3PO_4{\cdot}12H_2O$ and SiO_2 aiming to lower the sintering temperature thus improving chemical homogeneity. The best result was obtained with powder mixtures activated in Teflon containers with partial amorphisation of the reactants attained after milling for 70 h at a maximum of 300 rpm, without significant contamination. The microstructure consists of 300–500 nm agglomerates of smaller grains with size in the range 50–100 nm. Dense, single phase ceramics with submicrometric grain size were obtained from the activated mixture after sintering at 1050 °C for 10 h. The ionic conductivity of these ceramics is 2.5×10^{-3} S cm^{-1} at room temperature, and 0.24 S cm^{-1} at 300 °C. These values are higher than those obtained with non-activated solid state reaction samples and amongst the highest reported in the literature.

Keywords: Mechanical activation; Grain size; Electrical conductivity; NASICON; Sensors; Ionic conductivity; $Na_3Si_2(Zr,Y)_2PO_{12}$

1. Introduction

The $Na_{1+x}Zr_2Si_xP_{3-x}O_{12}$ solid solutions (NASICON) are well known fast sodium ionic conductors[1–4] with important electrochemical applications as CO_2 sensors[5,6] or Na^+ ion-selective electrodes.[7,8] The fabrication of homogeneous and pure NASICON ceramics is still challenging. The major problem is related to the formation of secondary P-rich amorphous phases which tend to segregate at the grain boundaries with a negative effect on the ionic transport properties. The traditional ceramic route usually implies the use of relatively high sintering temperatures which lead to an increase of the fraction of these amorphous phases and to sodium and phosphorous volatilisation with subsequent precipitation of monoclinic zirconia ($m$$ZrO_2$) crystallites.[8] The aim has been always to obtain very fine and reactive powders in order to keep the sintering temperature as low as possible. The sol–gel method was the first valid alternative to the standard ceramic route and is still largely used.[9] Recently, the use of reactive tetragonal-zirconia polycrystals (TZP) as zirconium precursor in a conventional high temperature solid-state reaction proved to be a valid approach to decrease the sintering temperature.[10] The main idea behind this approach is the use of a metastable precursor which is further from equilibrium than the $m$$ZrO_2$. This method yields dense ceramics with homogeneous microstructures, relatively small content of $m$$ZrO_2$, non-detectable amorphous phases at the boundaries and a high total conductivity, comparable to that of sol–gel-based ceramics.[10–12] In spite of the relatively good performance of these materials, they are not phase pure ($m$$ZrO_2$ is still present) and therefore further improvements may be achieved.

In all the reported methods, the solid state reaction is activated by a high temperature treatment, but the use of alternative methods such as the mechanical energy provided in a high energy ball mill may be envisaged. The mechanical

* Corresponding author. Tel.: +351-234-370263; fax: +351-234-425300.
E-mail address: framos@cv.ua.pt (F.M. Figueiredo).

0955-2219/$ – see front matter © 2004 Elsevier Ltd. All rights reserved.
doi:10.1016/j.jeurceramsoc.2004.02.019

energy is used to bring the precursors to a state far from equilibrium, usually amorphous, which then may be brought to the desired chemical constitution by heat treatment. The mechanical activation enhances the reactivity of solids, as well as mixing homogeneity and remarkably lowers the reaction temperature.[13,14] When the mechanical energy is enough to induce chemical reactions yielding the desired products, the process is known as mechanochemical synthesis. Many different materials have been successfully obtained via mechanical activation or mechanochemical synthesis, including, apart from many metal alloys, perovskite oxides such as $LaCrO_3$,[18] $CaTiO_3$[15] and $LaMnO_3$,[16] or strontium oxoferrates.[17] These powders are typically nanocrystalline and are thus particularly suitable to obtain ceramics with nanosized or submicrometric grains which may present some interesting advantages over the normal counterparts.[19]

The technique is simple, efficient and commercially attractive. It may present however a serious drawback related to contamination from the milling media (container and balls). Prolonged grinding should thus be avoided. The use of polymeric containers represents an alternative approach because although organic contamination can not be avoided, it can be easily removed by thermal treatment.[20]

This work represents an attempt to obtain nanosized NASICON powders by mechanical activation of precursors in a high energy planetary ball mill. Two types of experiments were designed with the intention of either minimise contamination or maximise the activation energy. Some preliminary electrical conductivity results obtained for ceramics with grains of the order of a few hundreds of nanometers (<500 nm) are reported.

2. Experimental

The nominal NASICON composition prepared in this work is $Na_3Si_2Zr_{1.88}Y_{0.12}PO_{11.94}$. High purity $(ZrO_2)_{0.97}(Y_2O_3)_{0.03}$ (Tosoh), $Na_3PO_4{\cdot}12H_2O$ (Merck) and SiO_2 (Merck) powders were initially ball milled with zirconia balls in ethanol during 2 h at 20 rotations per minute (rpm). After, the mixture was dried in air at 60 °C. Some water molecules of the sodium phosphate are lost during this process and the initial precursor becomes a mixture of $Na_3PO_4{\cdot}12H_2O$ and $Na_3PO_4{\cdot}8H_2O$. The mechanical activation of the precursors was carried out at room temperature without process control agents in two different experimental set-ups. Aiming to keep the level of contamination to a minimum, the reactants were dry grinded in a 100 cm^3 inner volume Teflon® container using a Restch 400 planetary ball mill operated at 200 and 300 rpm. Considerably higher mechanical energy was obtained in the second set of experiments using a Philips PW 4018 planetary ball mill operated at a constant 500 rpm. In this case, the reactants were in 45 cm^3 tetragonal zirconia polycrystals (TZP) containers. TZP balls with a diameter of 8 mm were used as grinding medium with a ball to powder weight ratio of 10:1, in both experiments. The grinding was interrupted at regular intervals (each 20 min) during the whole process to remove the powder from the wall of the containers.

At some of these intervals, small amounts of powder were removed for subsequent analysis by X-ray diffraction (XRD) using a Rigaku Geigerflex diffractometer (Cu Kα radiation, step 0.01°, 5 s/step) in order to identify compositional changes during grinding. The powder mixtures were also analysed in situ at high temperature by XRD (HTXRD) using an X'Pert MPD Philips diffractometer (Cu Kα X-radiation) with a curved graphite monochromator and a fix divergence slit of 1° in a Bragg–Brentano para-focusing optics configuration. This instrument is equipped with a high temperature chamber Anton-Parr GmbH HTK16 containing a Pt heating filament and a Pt–Pt/Rh(10%) thermocouple. The powder was dispersed in pure ethanol and deposited on the filament that acts also as sample holder. Intensity data were collected by the step counting method (step 0.05 and time 1 s) in the range $2\theta = 10$–40° at several temperatures with a heating rate of 10 K min^{-1}. The thermogravimetric (TGA) and differential thermal (DTA) analysis of the powders were carried out simultaneously with a constant heating rate of 5 K min^{-1} in a SETARAM TG-DTA LabSys instrument. The specific surface area was measured using a nitrogen adsorption Micromeritics Gemini 2370 BET surface area analyser, based on the Brunauer–Emmitt–Teller method (BET). The microstructure of the powders was evaluated by scanning and transmission electron microscopies (SEM and TEM) using a Hitachi S4100 SEM and a 300 kV Hitachi H-9000 TEM microscopes, both equipped with Rontec energy dispersive X-ray spectroscopy (EDS) detectors that were used to assess the chemical inhomogeneity of the samples. The powders were dispersed in ethanol and placed in a biological glass sample holder for the SEM, or in a perforated Cu greed for TEM. Several selected area electron diffraction (SAED) patterns were also collected to confirm XRD.

Disk shaped ceramic samples were obtained directly from the ground mixtures without any binder by uniaxially applying 100 MPa in a die with 1 cm in diameter. These samples were placed in a closed Pt crucible and sintered in air with an adequate cycle. The sintering curve was defined upon the TGA-DTA and XRD results. The grain size and general microstructural features of these ceramics were analysed by SEM on both as prepared and polished/thermally etched (at 825 °C for 30 min) ceramics. The phase composition was verified by XRD.

The electrical conductivity was measured in air by electrochemical impedance spectroscopy in the temperature range between 0 and 300 °C using a Hewlett Packard 4284A LCR meter. The spectra were collected in the frequency range between 20 Hz and 1 MHz with applied alternate amplitudes of 100 mV. Pt electrodes were previously painted onto the pellet's surfaces and then fired at 850 °C for 30 min to ensure the necessary electrical contacts.

3. Results and discussion

3.1. Mechanical activation of $Na_3PO_4{\cdot}12H_2O$–SiO_2–$(ZrO_2)_{0.97}(Y_2O_3)_{0.03}$ mixtures

Fig. 1 shows the XRD patterns obtained for non-activated and activated powders during different times. The pattern of the non-activated mixture reveals the presence of mainly the tetragonal zirconia ($t$$ZrO_2$) phase, $Na_3PO_4{\cdot}8H_2O$ (possibly also $Na_3PO_4{\cdot}12H_2O$) and monoclinic ($m$$ZrO_2$) zirconia. Note that $m$$ZrO_2$ is always present in the initial $(ZrO_2)_{0.97}(Y_2O_3)_{0.03}$ precursor as impurity. The amorphous SiO_2 is obviously not detected. The mechanical activation of the precursors for 50 h at 200 rpm leads to marked decrease in the intensity of the $t$$ZrO_2$ reflections, which is paired to a slight increase in those corresponding to $m$$ZrO_2$. This suggests that $t$$ZrO_2$ primarily amorphasises and subsequently transforms into the more stable room temperature monoclinic polymorph, probably loosing yttria. The increase of the grinding rotation to 300 rpm for additional 20 h further extended the $t$$ZrO_2$ → $m$$ZrO_2$ phase transition. On the other hand, milling is apparently rendering amorphous and/or decomposing the sodium phosphates and leading to the formation of a new phase, $Na_2HPO_4{\cdot}2H_2O$. Although the main reflections of $Na_3Si_2Zr_{1.88}Y_{0.12}PO_{11.94}$ are coincident with the other phases, the diffraction maximum at the characteristic $2\theta = 13.67^\circ$ for the (2 0 0) reflection is absent. The formation of NASICON is thus unlikely.

Similar patterns are obtained for mixtures activated at 500 rpm after 8 h. Again, NASICON is not formed. However, further increase of the activation time (up to 16 h) causes the complete amorphisation of the phosphates. On the other hand, a more pronounced increase of the fraction of $m$$ZrO_2$ is apparent, probably due to the considerably higher milling energy.

The increase of the $m$$ZrO_2$ fraction upon milling raises the issue of contamination. In fact, since the balls are predominantly composed of $t$$ZrO_2$, which usually transforms into $m$$ZrO_2$ during milling,[14] one must not exclude that at least a small part of the $m$$ZrO_2$ formed may actually result from the balls (and less likely the container walls) especially in the case of the 500 rpm experiment.

The SEM (Fig. 2) revealed that the activated powders have a relatively inhomogeneous microstructure consisting

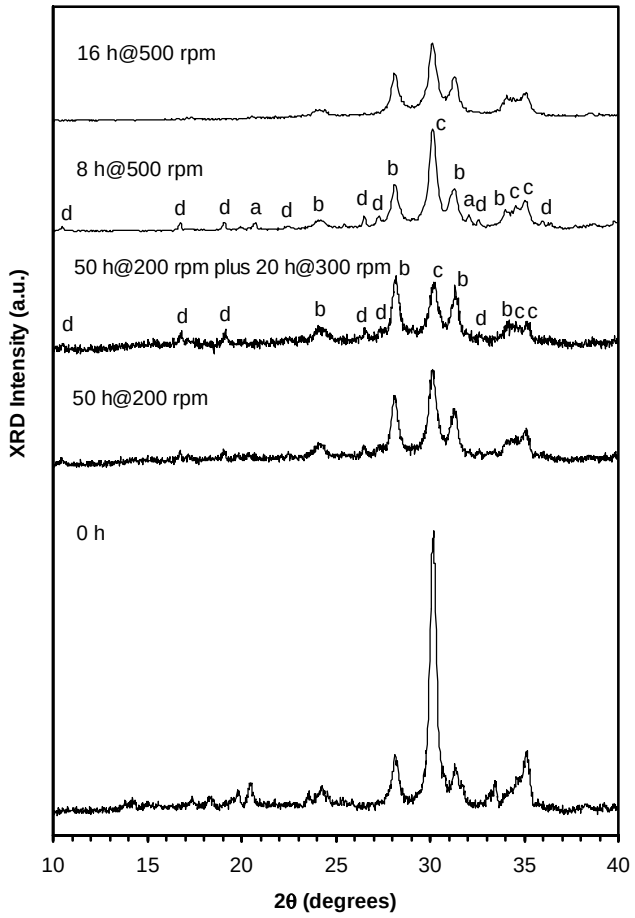

Fig. 1. XRD patterns of powders activated for different periods of time at 200 and 300 rpm in Teflon containers or at 500 rpm in zirconia containers. The peaks are indexed with letters corresponding to: (a) $Na_3PO_4{\cdot}8H_2O$ (JCPDS-ICDD file no. 37-0334); (b) $m$$ZrO_2$ (JCPDS-ICDD file no. 88-2390); (c) $t$$ZrO_2$ (JCPDS-ICDD file no. 88-1007); (d) $Na_2HPO_4{\cdot}2H_2O$ (JCPDS-ICDD file no. 70-0566).

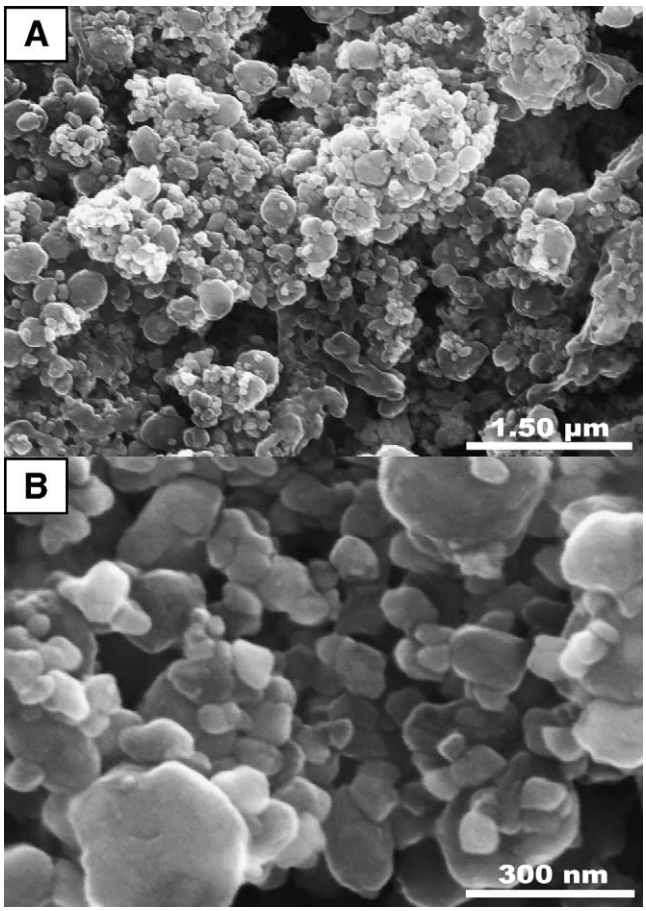

Fig. 2. SEM micrographs of a mixture mechanically activated at 200 rpm for 50 h followed by 20 h at 300 rpm in Teflon containers.

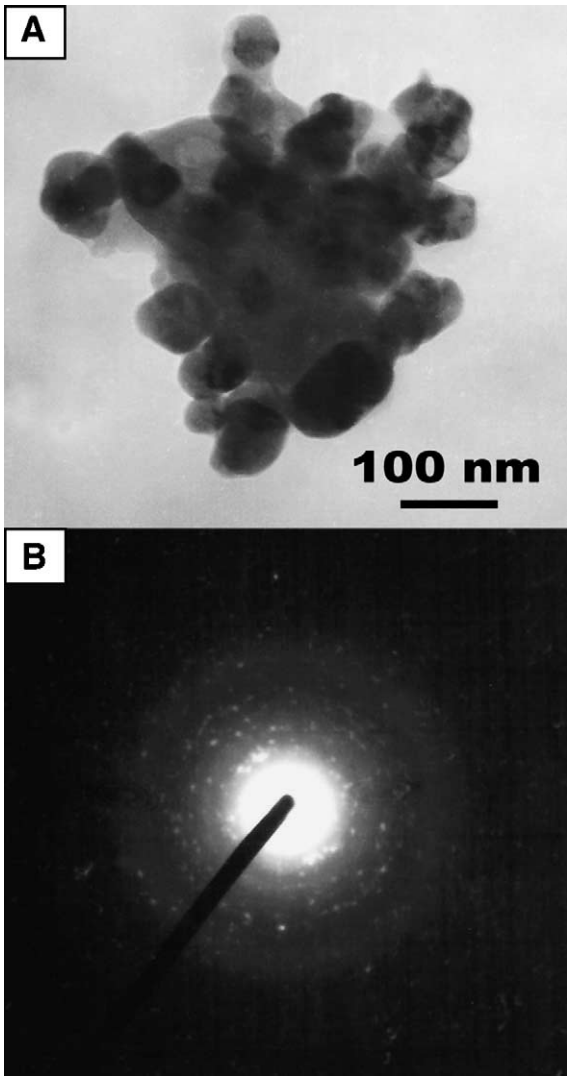

Fig. 3. TEM image (A) and corresponding SAED (B) of mechanically activated powders at 200 rpm for 50 h plus 20 h at 300 rpm in Teflon containers. The grain size is clearly lower than 100 nm.

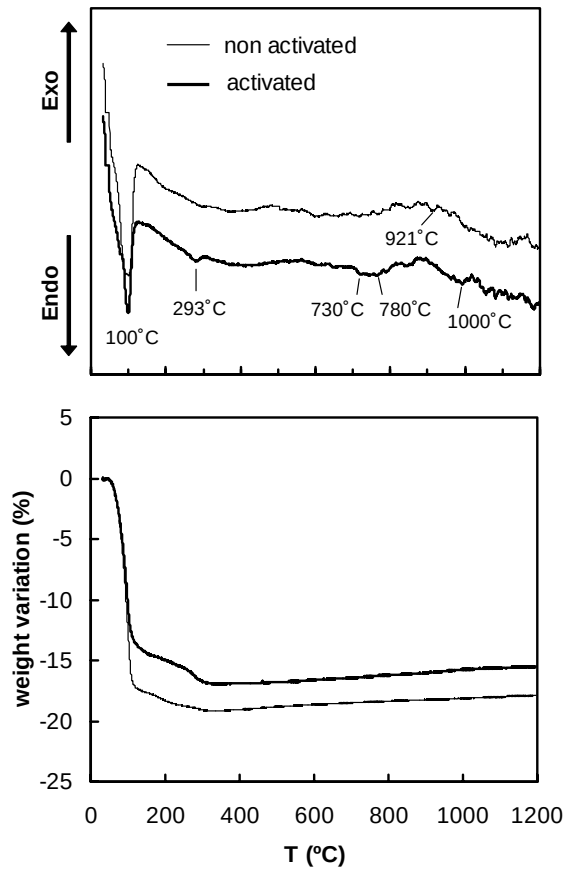

Fig. 4. Thermogravimetric and differential thermal analysis of non-activated and activated powders (50 h at 200 rpm followed by 20 h at 300 rpm).

of smaller grains with equivalent diameters ranging from about 40 to 200 nm and some larger particles with sizes close to 500 nm. The specific surface area of these powders was ≈4 m^2/g, which is much lower than for powders prepared by sol–gel[21] and certainly reflects the existence of agglomerates. Indeed, TEM (Fig. 3A) analysis further showed that the larger particles are actually agglomerates of smaller particles of nanometric size (100 nm or less). Several SAED patterns confirmed that these grains are predominantly amorphous after milling for 70 h. The diffraction spots are probably due to small zirconia crystallites dispersed within the amorphous phase, since single zirconia grains could not be detected.

3.2. High temperature treatment of activated powders

As noticed above, the mechanical energisation, under the conditions covered in this work, is insufficient to directly produce the desired NASICON phase via mechanochemical reaction 2nd hence a high temperature treatment was necessary. Fig. 4 shows the DTA-TGA curves for both a non-activated and an activated mixture at 200 rpm for 50 h plus 20 h at 300 rpm. The TGA is similar for both cases and shows that the weight losses occur at two temperature ranges. Most of the mass is lost up to ≈140 °C and this should be due to water losses associated to the hydrated sodium phosphate phases since a stiff endothermic peak is observed at 100 °C in the DTA curves. The lower variation observed for the activated mixture may be due to the release of water molecules associated to the decomposition of $Na_3PO_4{\cdot}8H_2O$ into $Na_2HPO_4{\cdot}2H_2O$ caused by milling. Above 150 °C the weight loss rate diminishes considerably until about 250 °C and then increases again up to ≈300 °C in the case of the activated mixture. The DTA results further indicate that this weight loss is associated to an endothermic reaction (peak at 293 °C in the DTA curve), probably due to decomposition of the anhydrous Na_2HPO_4 (expected to occur at 290 °C).[22] Nevertheless, the possibility that some of the weight loss is due to the decomposition of organic contamination from the container should not be discarded. No weight variations are apparent at temperatures higher than 300 °C, but the DTA reveals further differences with two

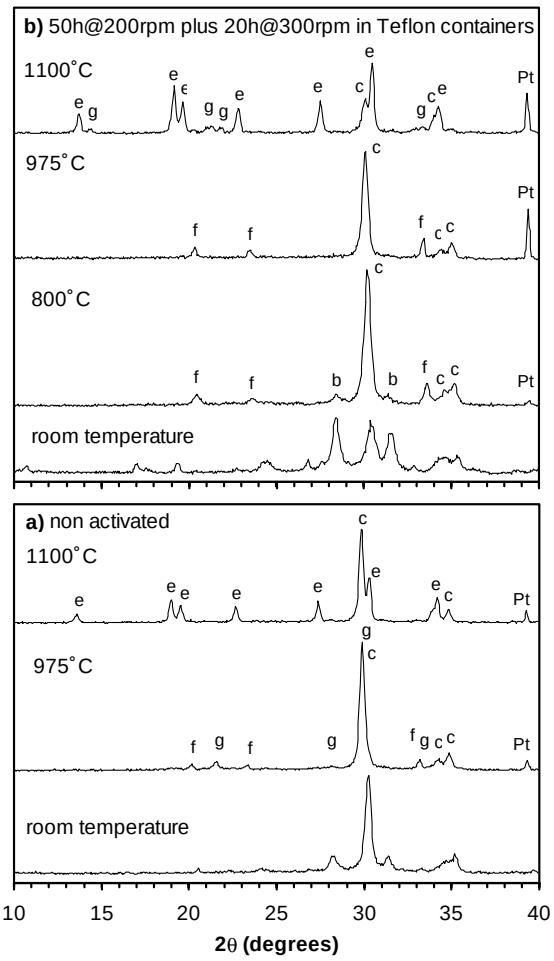

Fig. 5. XRD patterns obtained in situ at high temperature of the (a) non-activated precursors and (b) precursors activated for 50 h at 200 rpm plus 20 h at 300 rpm. The peaks are indexed with letters corresponding to: (a) $Na_3PO_4{\cdot}8H_2O$ (JCPDS-ICDD file no. 37-0334), (b) $m ZrO_2$ (JCPDS-ICDD file no. 88-2390), (c) $t ZrO_2$ (JCPDS-ICDD file no. 88-1007), (e) $Na_3Zr_2Si_2PO_{12}$ (JCPDS-ICDD file no. 84-1199), (f) Na_3PO_4 (JCPDS-ICDD file no. 30-1223) and (g) $Na_2ZrSi_2O_7$ (JCPDS-ICDD file no. 39-0209).

endothermic phenomena occurring in the activated powder at about 750–800 °C and ≈1000 °C. These are related to crystallisation or formation of new phases, e.g. NASICON.

The powder HTXRD patterns obtained in situ at relevant temperatures for activated and non-activated mixtures are shown in Fig. 5. The behaviour, similar up to 800 °C for both the activated and non-activated samples, mainly show the dehydration of the phosphate yielding the anhydrous tri-sodium phosphate Na_3PO_4. Considerable differences are, however, observed at higher temperatures. The 975 °C pattern of the non-activated sample reveals the presence of $Na_3ZrSi_2O_7$, probably preceded by formation of sodium silicates (Na_3SiO_3 or $Na_2Si_2O_5$) which in turn reacted with the zirconia. The formation of this compound might explain the small endothermic peak at ≈920 °C observed in Fig. 4. No crystalline phases in the ternary Na_2O–SiO_2–P_2O_5 could be identified, but their presence in an amorphous state is likely since the *liquidus* temperature is close to 900 °C in the compositional range of interest.[23] The onset of the reflections of NASICON occurs above this temperature, paired to a significant decrease of the $t ZrO_2$ peaks and with full reaction of Na_3PO_4 and $Na_3ZrSi_2O_7$, which peaks can no longer be identified. The present results suggest two competitive reactions occurring with zirconium consumption, one leading to the desired NASICON and the other to $Na_3ZrSi_2O_7$, the latter compound being more stable at lower temperatures. Note that the $m ZrO_2 \rightarrow t ZrO_2$ phase transition occurs as temperature increases, with full conversion eventually achieved at 975 °C.

The patterns obtained with the activated powders show that Na_2HPO_4 crystallises at temperatures lower than 800 °C, in agreement with the endothermic heat flux spanning from 700 to 800 °C observed in Fig. 4. The $Na_3ZrSi_2O_7$ peaks are present only in the 1100 °C pattern (probably associated to the endothermic peak observed in the DTA curve at approximately 1000 °C), which may indicate that the mechanical activation hinders the formation of this silicate. On the other hand, while the intensities of the zirconia reflections are lower than those of NASICON when the powders are not mechanically activated, the opposite occurs for the activated powders suggesting the former to be more reactive. It thus seems that the mechanical activation promotes the kinetics of the NASICON formation reaction but has a retarding effect on the crystallisation of $Na_3ZrSi_2O_7$.

3.3. Sintering behaviour

The DTA/TGA and XRD results were used to obtain NASICON ceramics using directly the activated and non-activated precursor mixtures thus avoiding intermediate calcination steps which degrade the sinterability of the powders. The samples were sintered in air using a two steps cycle, firstly at 600 °C for 1 h and then at 1000 or 1050 °C for 10 h, always with a heating rate of 2 K min^{-1}. Attempts to obtain dense samples from the powders activated at 500 rpm in zirconia pots failed. The NASICON phase could indeed be obtained but significant levels of monoclinic zirconia were also present. Therefore, no additional results on these samples are provided in this and the next sections.

Fig. 6 shows XRD results for a NASICON ceramic sample obtained from mechanically activated precursors (200 rpm for 50 h plus 20 h at 300 rpm) sintered at 1050 °C for 10 h. Within the detection limit of the diffractometter, the sample is almost single phase with traces of sodium phosphate but without $m ZrO_2$. The results now presented confirm the kinetic limitations as the reason for incomplete NASICON formation evidenced by Fig. 5. This result was obtained at 1100 °C during a much shorter annealing time (about 15 min). Actually, NASICON can be formed at temperatures as low as 1000 °C (Fig. 6), although evidence

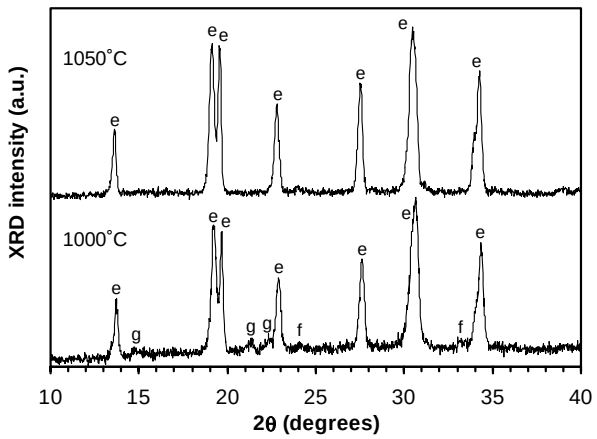

Fig. 6. XRD patterns of dense ceramics obtained from activated mixtures and sintered at different temperatures for 10 h. The peaks are indexed with letters corresponding to: (e) $Na_3Zr_2Si_2PO_{12}$ (JCPDS-ICDD file no. 84-1199), (f) Na_3PO_4 (JCPDS-ICDD file no. 30-1223) and (g) $Na_2ZrSi_2O_7$ (JCPDS-ICDD file no. 39-0209).

for incomplete reaction of $Na_3ZrSi_2O_7$ and Na_3PO_4 is still present after annealing for 10 h.

If, as shown, the phase composition of ceramics obtained from activated and non-activated precursors is not very different, the microstructure, however, is. Fig. 7 illustrates these differences. The first and obvious one is the densification. While the non-activated sample shows a considerable level of porosity (Fig. 7A), the activated sample is almost 100% dense (Fig. 7B) with a geometric density of 3.24 g cm^{-3}. To attain such low porosity, the non-activated samples must be sintered at about 1220 °C.[10,11] This means that dense NASICON ceramics may be obtained at temperatures which are 150–200 °C lower than those needed for normally prepared materials. The second remarkable difference is the ability to retain in the activated ceramics the small grain size of the powdered precursors. Fig. 7C reveals clear submicrometric microstructure with a bimodal grain size distribution. The smaller grains have a diameter of 100–200 nm while in the larger ones is of the order of 500 nm. Typical grains in dense non-activated samples sintered at ≈1200 °C have an equivalent grain diameter larger than 1 μm.[10–12]

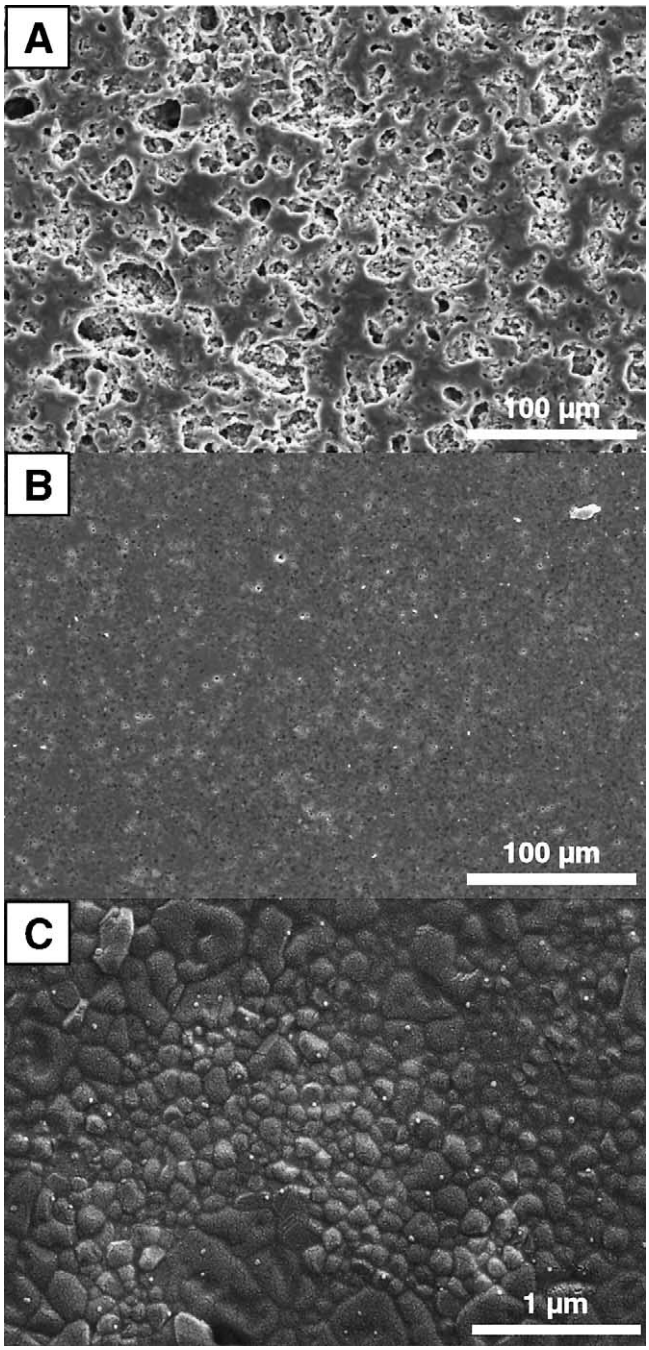

Fig. 7. SEM micrographs of NASICON ceramics sintered at 1050 °C for 10 h: (A) ceramics obtained from non-activated precursors; (B and C) ceramics obtained from precursors activated for 16 h at 500 rpm in zirconia containers.

3.4. Electrical conductivity

Fig. 8 shows typical impedance spectra at 0 and 25 °C of an activated (200 rpm for 50 h plus 20 h at 300 rpm in Teflon containers) ceramic sample sintered at 1050 °C. Since only part of the grain boundary semi-circle can be identified, the separation of both grain and grain boundary contributions to the total impedance is not possible at the measuring temperatures covered in this work. Although measurements at temperatures lower than 0 °C are fundamental to complete the electrical characterisation of these ceramics, it is nonetheless apparent that the grain boundary contribution is considerably larger than the bulk one. This is in good agreement with the previously reported resistive nature of the grain boundaries.[12]

The impedance plots, however, enable the determination of the total electrical conductivity in a sufficiently wide temperature range for a meaningful comparison of the performance of activated and non-activated ceramics. These values are shown in Arrhenius coordinates in Fig. 9. The room temperature conductivity, assumed to be essentially ionic, of the

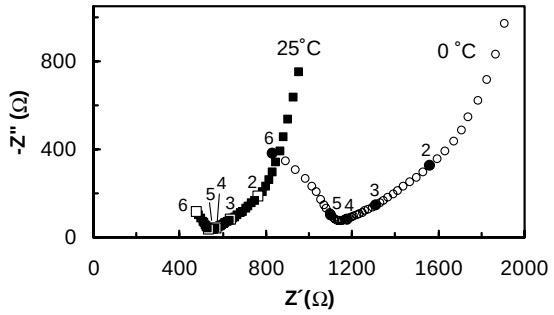

Fig. 8. Nyquist plots in air at room temperature of NASICON ceramics obtained from powders mechanically activated during 50 h at 200 rpm plus 20 h at 300 rpm and sintered at 1000 °C for 10 h. Numbers indicate log 1ϕ of the frequency.

activated sample is 2.5×10^{-3} S cm^{-1} while it increases to 0.24 S cm^{-1} at 300 °C. These values are considerably higher than those obtained with the non-activated material (open circles in Fig. 9), which are of the order of 1.7×10^{-3} S cm^{-1} and 0.15 S cm^{-1}, respectively at 25 and 300 °C. The activation energy, ≈29 kJ mol^{-1}, indicates similar conduction mechanisms for both ceramics. Whether this improvement is due to a higher degree of chemical homogeneity, or to the modification of the nature of the grains or grain boundaries, remains to be clarified.

The conductivity and corresponding activation energy values for the activated ceramics are comparable or even better than those, shown in Fig. 9, reported for ceramics obtained from sol–gel precursors method. Indeed, the dashed line in Fig. 9 represents the, to our knowledge, best conductivity results for $Na_3Si_2Zr_2PO_{12}$ ceramics sintered at 1250 °C and with considerable larger grain size.[24]

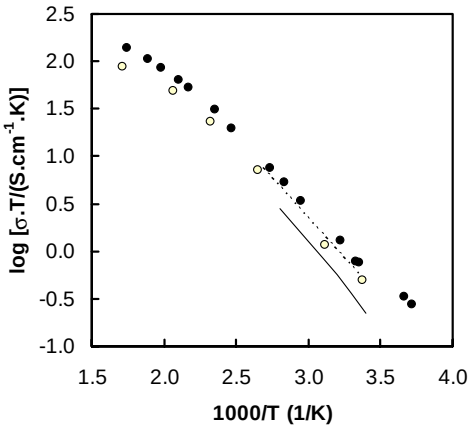

Fig. 9. Arrhenius-type plot of total conductivity as function of absolute temperature of several NASICON samples: (●) $Na_3Si_2Zr_{1.88}Y_{0.12}PO_{11.94}$ sintered at 1050 °C/10 h using precursors activated at 200 rpm for 50 h followed by 20 h at 300 rpm; (○) $Na_3Si_2Zr_{1.88}Y_{0.12}PO_{11.94}$ sintered at 1220 °C/40 h using non-activated precursors;[12] solid and dashed lines correspond, respectively, to data for $Na_3Si_2Zr_2PO_{12}$ ceramics sintered at 1200 °C[8] and 1250 °C obtained following a sol–gel route.[24]

4. Conclusions

The high energy grinding of powdered precursors is a promising route to obtain single phase NASICON-based materials. The advantages over the classical ceramic route appear to be related to a significant improvement of the reaction kinetics due to the smaller grain size (<100 nm) of the activated powders and a modification of the thermodynamic properties of the reactants. NASICON is only formed at temperatures higher than 1000 °C either when mechanically activated or non-activated precursors are used. The best results were obtained from a combination of moderate milling energies (200–300 rpm in a planetary ball mill) using organic (Teflon) containers with zirconia balls. Harsher milling conditions (500 rpm), used in an attempt to directly synthesise NASICON via mechanochemical reactions, lead, instead, to an increase of the fraction of monoclinic zirconia in the precursors mixture.

Dense NASICON ceramics may be obtained from uniaxially pressed activated powders sintered at temperatures as low as 1000 °C for 10 h. The Na_3PO_4 impurities present in this sample fully react at 1050 °C yielding almost single phase materials. This temperature is 150–200 °C lower than the normally needed. Given the rather mild sintering conditions, the small grain size of the precursors is partially retained and the ceramics microstructure consists of smaller 100–200 nm grains side by side with larger ones (500 nm), probably as the result of the agglomerates.In spite of the large grain boundary density, preliminary electrical measurements have shown that the total electrical conductivity measured for these samples (2.5×10^{-3} S cm^{-1} at 25 °C) is higher than for the non-activated samples and comparable to the best values reported up to now for sol–gel-based ceramics.

Acknowledgements

This work was supported by the FCT, Portugal (POCTI program and project BD/6594/2001).

References

1. Hong, H. Y. P., Crystal structures and crystal chemistry in the system $Na_{1+x}Zr_2Si_xP_{3-x}O_{12}$. *Mater. Res. Bull.* 1976, **11**, 173–182.
2. Goodenough, J. B., Hong, H. Y. P. and Kafalas, J. A., Fast Na^+-ion transport in skeleton structures. *Mater. Res. Bull.* 1976, **11**, 203–220.
3. Boilot, J. P., Salaine, J. P., Desplanches, G. and Le Potier, D., Phase transformations in $Na_{1+x}Si_xZr_2P_{3-x}O_{12}$ compounds. *Mater. Res. Bull.* 1979, **14**, 1469–1477.
4. Ahmad, A., Wheat, T. A., Kuriakose, A. K., Canaday, J. D. and McDonald, A. G., Dependence of the properties of NASICONS on their composition and processing. *Solid State Ionics* 1987, **24**, 89–97.
5. Maruyama, T., Sasaky, S. and Saito, Y., Potentiometric gas sensor for carbon-dioxide using solid electrolytes. *Solid State Ionics* 1987, **23**, 107–112.
6. Kida, T., Miyachi, Y., Shimanoe, K. and Yamazoe, N., NASICON thick film-based CO_2 sensor prepared by a sol–gel method. *Sens. Actuators B* 2001, **80**, 28–32.

7. Caneiro, A., Fabry, P., Khireddine, H. and Siebert, E., Performance characteristics of a sodium super ionic conductor prepared by sol–gel route for sodium ion sensors. *Anal. Chem.* 1991, **63**, 2550–2557.
8. Khireddine, H., Fabry, P., Caneiro, A. and Bochu, B., Optimization of NASICON composition for Na^+ recognition. *Sens. Actuators B* 1997, **40**, 223–230.
9. Perthuis, H. and Colomban, Ph., Well densified NASICON type ceramics, elaborated using Sol–Gel process and sintering at low temperatures. *Mater. Res. Bull.* 1984, **19**, 621–631.
10. Fuentes, R., Franco, J. and Marques, F. B., Synthesis and properties of NASICON prepared from different zirconia-based precursors. *Bol. Soc. Esp. Cer. Vidrio* 1999, **38**(6), 631–634.
11. Fuentes, R. O., Figueiredo, F. M., Marques, F. M. B. and Franco, J. I., Processing and electrical properties of NASICON prepared from yttria-doped zirconia precursors. *J. Eur. Ceram. Soc.* 2001, **21**, 737–743.
12. Fuentes, R. O., Figueiredo, F. M., Marques, F. M. B. and Franco, J. I., The influence of microstructure on the electrical properties of NASICON. *Solid State Ionics* 2001, **140**, 173–179.
13. Avvakumov, E., Senna, M. and Kosova, N., *Soft Mecahnochemical Synthesis: A Basis for New Chemical Technologies*. Kluwer Academic Publishers, 2001, Chapters 6 and 7.
14. Suryanarayana, C., Mechanical alloying and milling. *Prog. Mater. Sci.* 2001, **46**, 1–184.
15. Mi, G., Murakami, Y., Shindo, D. and Saito, F., Mechanochemical synthesis of $CaTiO_3$ from a CaO–TiO_2 mixture and its HR-TEM observation. *Powder Technol.* 1999, **105**, 162–166.
16. Zhang, Q. and Saito, F., Mechanochemical synthesis of $LaMnO_3$ from La_2O_3 and Mn_2O_3 powders. *J. Alloys Compd.* 2000, **297**, 99–103.
17. Tsuchida, T. and Morita, N., Formation of ternary carbide Co_6W_6C by mechanical activation assisted solid-state reaction. *J. Eur. Ceram. Soc.* 2001, **22**, 2401–2407.
18. Berbinni, V. and Marini, A., Solid state synthesis of strontium oxoferrates from the mechanically activated system $SrCO_3$–Fe_2O_3. *Mater. Res. Bull.* 2002, **37**, 221–234.
19. Schoonman, J., Nanoionics. *Solid State Ionics* 2003, **157**, 319–326.
20. De Castro, C. and Mitchell, B., The use of polymeric milling media in the reduction of contamination during mechanical attrition. *J. Mater. Res.* 2002, **17**(12), 2997–2999.
21. Khireddine, H., *Etude des Perfomances de Capteurs Potentiometriques. A Ions Sodium Utilisant des Membranes de NASICON*. Ph.D. thesis, Institut National Polytechnique de Grenoble, Grenoble, France, 1992.
22. Taylor, P., Tumaine, P. R. and Bailey, M. G., Sodium oxide-phosphorous (V) oxide-water phase-diagram near 300-degrees-C—equilibrium solid-phases. *Inorg. Chem.* 1979, **18**(11), 2947–2953.
23. *Phase Diagrams for Ceramists, Figs. 533–536*. American Chemical Society, Columbus, E.U.A., 1964.
24. Colomban, Ph., Orientational disorder, glass/crystal transition and superionic conductivity in NASICON. *Solid State Ionics* 1986, **21**, 97–115.